The International Journal of Advanced Manufacturing Technology (2020) 106:3071–3080
https://doi.org/10.1007/s00170-019-04871-z

ORIGINAL ARTICLE

Experimental investigations on magnetic abrasive finishing of Ti-6Al-4V using a multiple pole-tip finishing tool

Yebing Tian[1] · Chen Shi[1] · Zenghua Fan[1,2] · Qiang Zhou[1]

Received: 9 April 2019 / Accepted: 19 December 2019 / Published online: 2 January 2020

Abstract
Surface finishing plays a critical role in product manufacturing. This paper aims to evaluate the magnetic abrasive finishing (MAF) process in achieving nano-finishing on Ti-6Al-4V workpiece. An improved finishing tool–integrated multiple pole-tip is fabricated to perform the surface finishing of Ti-6Al-4V workpieces. Finite element analysis of the variation of magnetic field intensity in the finishing region demonstrates obvious formation of magnetic brush based on the simulation model. The simulation results are confirmed by experimental measurements, where it shows a good agreement. Finishing experiments for Ti-6Al-4V workpieces are carried out using an established platform, aiming to investigate the effects of varying the spindle rotational feed, the rotary table speed, and the working gap on surface roughness (R_a). The surface roughness of 0.073 μm was achieved from the initial 1.195 μm based on the finishing parameters of 900-rpm spindle rotational speed, 160 r/min rotary table speed, and 0.7-mm working gap, which improved by over 94%. The surface quality was improved significantly with scratch reduction.

Keywords Multiple pole-tip · Magnetic brush · Finishing tool · Ti-6Al-4V workpiece · Surface roughness

1 Introduction

Titanium alloys has widespread applications in the shipbuilding industry, aerospace industry, and automotive manufacturing owing to the outstanding corrosion resistance, good durability, and low toxicity [1, 2]. To satisfy the stringent requirements of industries, the available finishing processes like grinding, lapping, magnetic field–assisted finishing (MFAF), laser polishing, etc. are employed for finishing operations [3–7].

The machinability of titanium alloys aroused considerable interest in the precision finishing process. Beaucamp et al. developed a shape-adaptive grinding device with small grinding pellets for post-finishing of Ti-6Al-4V workpiece manufactured by electron beam melting (EBM) and selective laser sintering (SLS). The surface was smoothed down to 10-nm roughness (R_a) from initial 4–5 μm by using diamond abrasive with three different sizes [8]. Revankar et al. focused on optimizing the machining parameters including burnishing feed, burnishing force, and number of passes during ball burnishing of titanium alloy [9]. Axinte et al. investigated the feasibility of using belt finishing for components made of Ti-6Al-4V alloys based on experimental approaches. A required surface with three different fabricated textures was achieved by varying cutting parameters and the finishing strategy [10]. Similarly, a robot-assisted belt grinding process for titanium alloys was characterized and analyzed using a plowing force model [11]. To improve the corrosion resistance of the workpiece, an electrochemical grinding system that organized an oxide film on the processed surface by applying short DC pulses was established [12]. In addition, some researchers also reported chemical mechanical polishing [13, 14] and electrolytic polishing [15, 16] for finishing titanium alloys.

Many types of MFAF are available in fields of precision machining because of good flexibility and easy controllability [17, 18]. Several processes, like magnetic float polishing (MFP) [19], magnetorheological abrasive flow finishing (MRAFF) [20], magnetic abrasive finishing (MAF) [21], and magnetorheological finishing (MRF) [22], describe the

✉ Zenghua Fan
zhfan@sdut.edu.cn

[1] School of Mechanical Engineering, Shandong University of Technology, 266 Xincun West Road, Zibo, Shandong 255049, People's Republic of China

[2] Shandong Provincial Key Laboratory of Core Tire Mold Technology, Gaomi 261500, People's Republic of China

most common ones. Barman et al. designed a MFAF tool by mixing MR fluids with abrasives as the finishing media to fulfill nano-level polishing of bio-titanium alloys [23, 24]. Zhou et al. evaluated the capacity of MAF process of titanium sheets assisted by extra ultrasonic vibration and reported that the efficiency is 40% improvement under ultrasonic magnetic abrasive finishing [25]. Parameswari et al. explored the critical parameters of the MRF process in achieving nano-finishing on Ti-6Al-4V flat discs. The final surface roughness with 95 nm was achieved by experimental investigations [26]. Yamaguchi et al. described MAF finishing mechanism for cutting tools with rake, flank, and nose surfaces, and the tool life is improved by 50–60% in milling of Ti-6Al-4V [27, 28]. However, few researchers focused on the finishing tool developments with multi-magnetic pole in Ti-6Al-4V finishing.

In the present study, an improved tool is developed for MAF process to polish Ti-6Al-4V alloy surface. The structure of the finishing tool and the processing principle are described firstly. Then, simulation model based on finite element analysis is employed to evaluate the magnetic field distributions of 64 magnetic poles. The simulated results are verified using experimental measurements. Finally, experimental and analytical investigations on surface finishing of Ti-6Al-4V alloy by MAF are performed. The effects of varying the spindle rotational feed, the rotary table speed, and the working gap on surface roughness are quantitatively analyzed. The optical microscope and scanning electron microscope (SEM) are adopted to evaluate the surface finishing quality.

2 Design of finishing tool

2.1 Basic structure

A schematic representation of the designed finishing tool is shown in Fig. 1. The round tray is fixed together with the rotary table by four mounting holes so that a required speed rotation is delivered. Sixty-four holes, which are arranged in three circles, are fabricated for permanent magnet placement on the bottom of the round tray. A baffle manufactured from acrylic plate is employed for abrasive media placement. It is expected that the required magnetic field is generated by the action of permanent magnets. Notably, several configurations are structured conveniently by varying the arrangements of north (N) and south (S) poles during finishing tasks. Accordingly, the control of the finishing media is achieved because the magnetic force lines are changing. The finishing tool integrated with multiple poles contributes to improve the finishing efficiency. The developed finishing tool has attractive advantages of high operability and easy replacement.

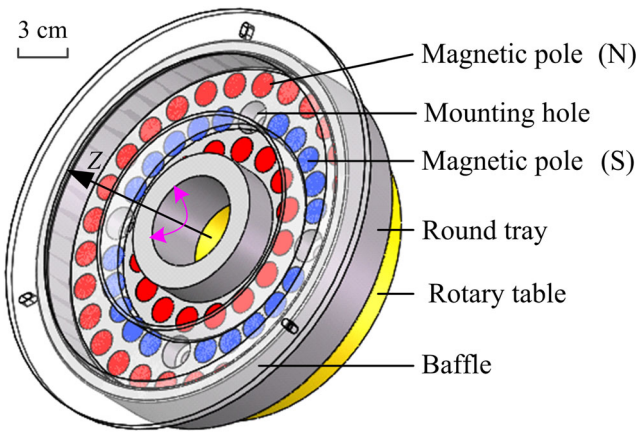

Fig. 1 Schematic illustration of the finishing tool configuration

2.2 Processing principle

The proposed magnetic abrasive finishing process for Ti-6Al-4V plate finishing based on the designed finishing tool is shown in Fig. 2. The north (N) poles are placed in the outer and inner circles, and the middle circle is arranged with south (S) poles. The desired magnetic field is formed for attracting the finishing abrasives. The iron particles mixed with SiC particles are attracted along the magnetic field lines as a finishing brush. The spindle and rotary table are adopted to achieve the rotation of workpiece and magnetic poles, respectively. This causes relative friction between the workpiece surface and the magnetic brush, thereby realizing effectively the material removal.

3 Magnetic field analysis

The magnetic characterization of the developed finishing tool plays an important role in accomplishing surface finishing. Magnetic pole distribution of N-S-N is arranged in the two-dimensional (2D) simulation model of ANSYS Maxwell environment. N38 NdFeB permanent magnets with Φ14 mm × 10 mm are adopted in the simulation model. Materials of the round tray and baffle are defined as 1008 steel and plexiglass, respectively. Materials of the simulation model definition are consistent with the fabricated finishing tool using in experimental tests. The distribution of formed magnetic field lines is shown in Fig. 3. In the air medium, the magnetic field lines pass from N pole-tip to S pole-tip. Accordingly, a closed loop is formed when it returns to the bottom of N pole through the round tray. A flexible fixed abrasive will be generated in each loop because of the action of applied magnetic field. In the 3D model, protrusions are formed as a circle between the N poles and the S poles. The multi-protrusion contributes to improve the finishing efficiency, where the magnetic brush has more contact with the surface in finishing processes.

To verify the effectiveness of the proposed simulation model, contrast experiments are performed between the simulation

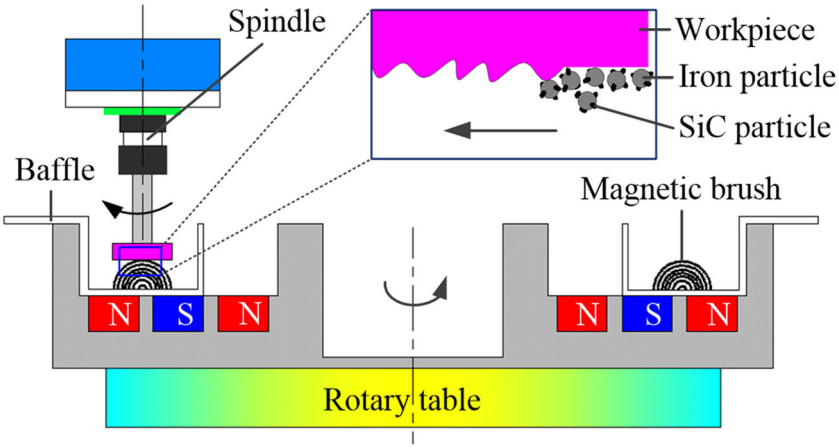

Fig. 2 Processing principle of the finishing tool

results and experimental tests. The field intensity distributions along line 1 and line 2 are investigated using three-dimensional (3D) simulation approaches. The starting point of line 1 is set on the center point of four poles, and the N pole-tip is set as the starting point of line 2. Figure 4 shows the magnetic field intensity change with varying distance from the starting point. The field intensity was inverse relation with the gap size. The maximum magnetic intensity of 0.054 T and 0.22 T is obtained at the starting point of line 1 and line 2, respectively. This is because magnetic lines dissipate when the distance increases. Measurement tests, using a Gauss meter (Model No.: GM500), were implemented to examine the variation in field intensity as comparisons to simulation results. Numbers of 11 points with the interval of 0.5 mm are adopted as the measurement points, as shown in Fig. 4. The results indicate that the magnetic field intensity dropped significantly with the increase of gap size. And the variation tendency of experimental measurements is consistent with simulation results. The measured values were 0.052 T and 0.18 T at the starting point of line 1 and line 2, respectively. This indicates that the simulation method is effective for the magnetic field analysis.

4 Experiments

4.1 Finishing media preparation

Carbonyl iron particles in 250-μm diameter and SiC abrasives in 150-μm diameter are employed as the finishing media preparation. Lubricant oil serves binding function for the mixture of iron particles and SiC abrasive. Then, the lubricant oil was added to the mixture and vigorous stirring is continued for 30 min further. This results in a uniform dispersion of the prepared mixture. Figure 5 shows the photograph and the SEM image of the prepared finishing media.

4.2 Experimental setup and conditions

A customized platform, including primarily a CNC machine center (VKN640), a rotary table, and a designed finishing tool, was established to perform the finishing investigations, as illuminated in Fig. 6. The maximum spindle rotational speed of the established platform is 12,000 rpm. The workpiece is connected to the spindle.

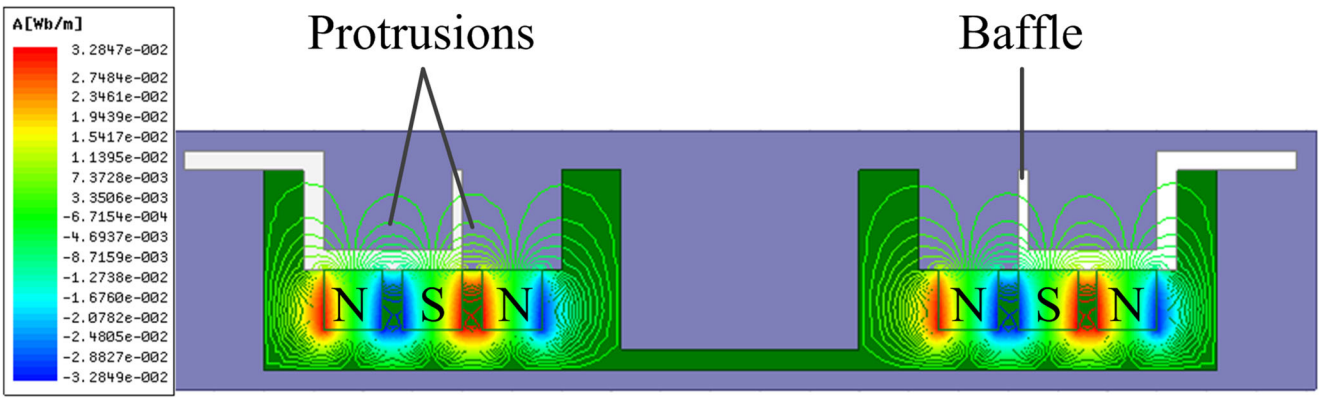

Fig. 3 Distributions of magnetic field lines using N-S-N mode

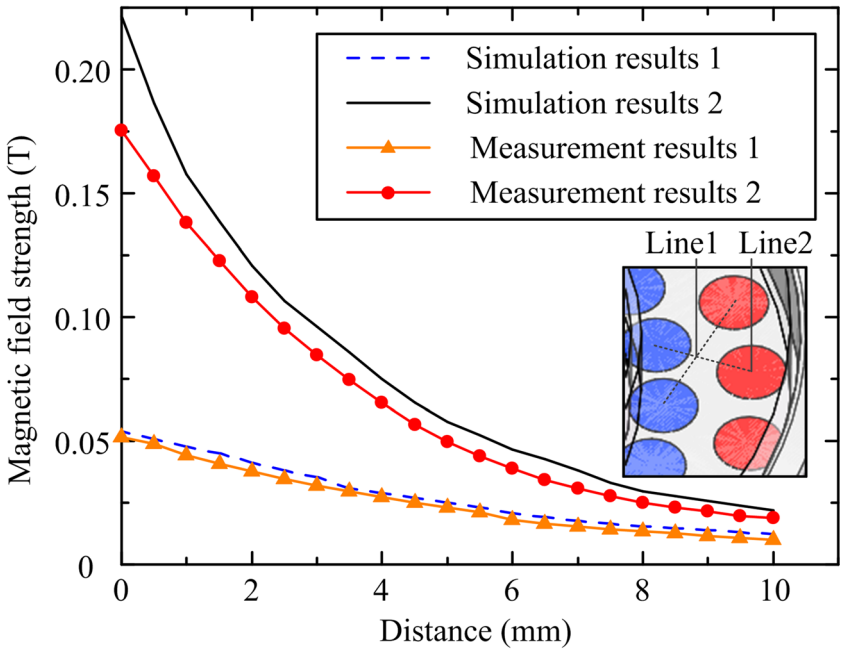

Fig. 4 Comparisons between simulation and experimental measurement

The designed finishing tool, including a round tray, a baffle, and 64 poles, was held in the rotary table. Circle protrusions were formed under the N-S-N mode of the magnetic pole arrangements when the finishing media were placed on a baffle with thickness of 5 mm. The gap size is changed conveniently between the magnetic pole-tip and the workpiece surface by adjusting the spindle movement in *Z* direction.

The detailed experimental conditions are listed in Table 1. Flat Ti-6Al-4V of size 13 × 10 × 4 mm are prepared for the finishing experiments. An initial surface roughness of ~ 1.2 μm is prepared via #60 sand paper grinding. Three rotational speeds of 300, 500, and 700 rpm and the rotary table speed of 100, 130, and 160 r/min were employed for finishing experiments. The working gap was set to 0.7, 1.1, and 1.5 mm between the magnetic role and the workpiece for finishing investigations, respectively.

5 Results and discussions

5.1 Surface roughness

To investigate the finishing capability of the developed finishing tool, extensive experiments were conducted to examine the effect of finishing time on surface roughness (R_a) value of the workpiece. The effects of varying spindle rotational speed, rotary table speed, and gap size on surface roughness are investigated independently. The variation of surface roughness is measured every 10 min using a commercial

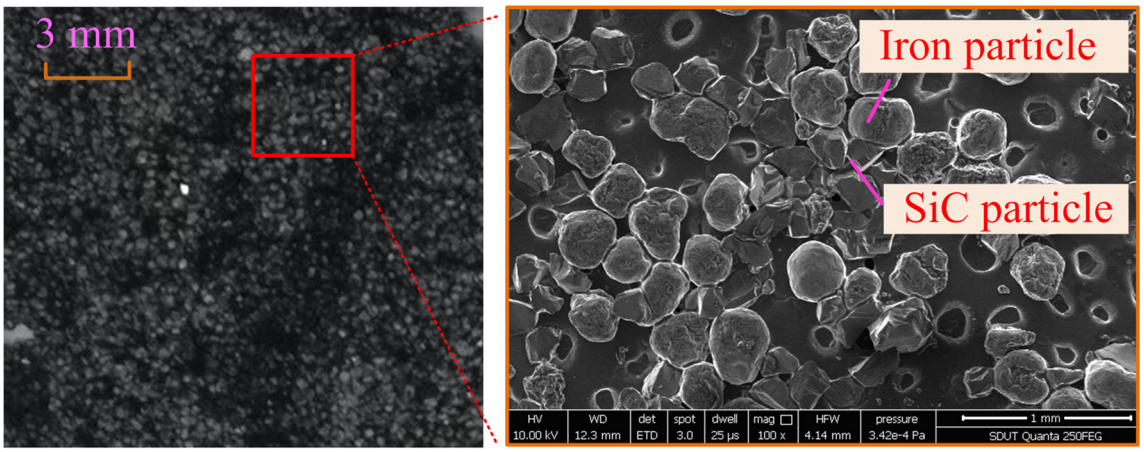

Fig. 5 Finishing media

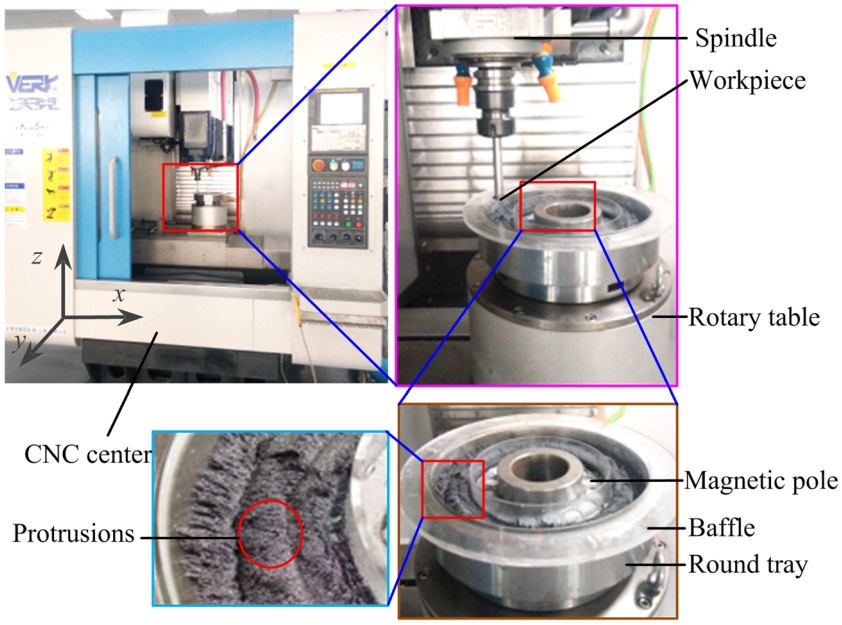

Fig. 6 Experimental setup

roughness tester (TR200). The total mass of the finishing media was 100 g.

5.1.1 Varying spindle rotational feed

The spindle rotational speed is one of an important factor affecting the surface roughness. Figure 7 shows the time-dependent variation in surface roughness with three different spindle rotational feeds. The rotary table speed is 160 r/min and the working gap is 0.7 mm. The surface roughness values are reduced gradually with finishing time of 90 min, especially in the initial stage. Surface roughness values of 0.127, 0.091, and 0.073 μm were obtained under the spindle rotational feeds of 300, 500, and 700 rpm, respectively, after 90-min finishing. The surface roughness of 0.073 μm on the finished surface was obtained from initial value of 1.195 μm under the action of 700-rpm spindle rotational feed, which improved by over 94%.

Table 1 Experimental conditions

Items	Parameters
Workpiece material	Ti-6Al-4V
Initial roughness (μm)	~ 1.2
Spindle rotational speed (rpm)	300, 500, 700
Rotary table speed (r/min)	100, 130, 160
Working gap (mm)	0.7, 1.1, 1.5
Lubricant oil	No. 64
Carbonyl iron particle size (μm)	250
SiC particle size (μm)	150
Weight ratio (iron:SiC)	9:1

5.1.2 Varying rotary table speed

Figure 8 shows the surface roughness values with various rotary table feeds at different finishing time. Three rotation speeds, including 100, 130, and 160 r/min, are employed for finishing trail. The spindle rotational speed is 700 rpm and the working gap size is 0.7 mm. It is shown clearly that the surface roughness dropped with finishing process proceeding. The greater rotation speed resulted in the faster decline in surface roughness. The values were reduced to 0.169 μm, 0.138 μm, and 0.073 μm from the initial 1.2 μm under three rotary table speed action in 90 min, respectively, and became finally stable. According to Preston's equation [29], the material removal is proportional to the velocity, which is correlated with the surface roughness drop. A lower rotational feed reduces the velocity and decreases the finishing efficiency.

5.1.3 Varying gap size

To examine the effects of working gap on surface roughness, finishing experiments were further conducted based on the spindle rotational speed of 700 rpm and rotary table speed of 160 r/min. A lower roughness value is observed in small working gap, as illustrated in Fig. 9. It is evident that the surface roughness value dropped significantly in the initial finishing stage with 0.7-mm gap size. The final surface roughness values of 0.073, 0.102, and 0.205 μm were obtained under 0.7-, 1.1-, and 1.5-mm gap size, respectively. The filed intensity decreased with the increase of the gap size, which caused a higher normal and shearing force with a smaller working gap [30].

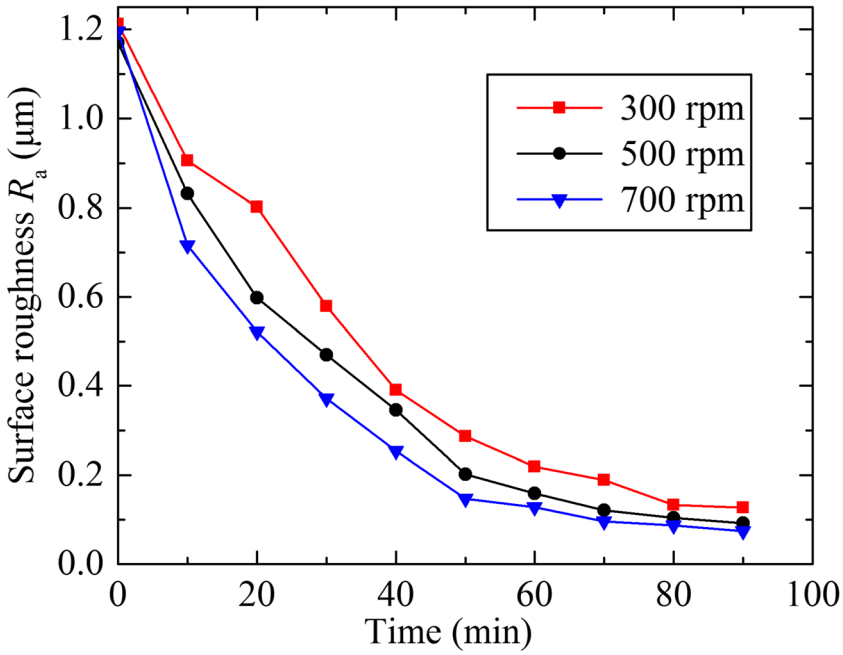

Fig. 7 Surface roughness variation with different spindle rotational feeds

5.2 Surface observations

To further explore the processing capability, surface observations were carried out under the processing conditions of 700-rpm spindle rotational speed, 160 r/min rotary table speed, and 0.7-mm working gap, which exhibited the best surface quality in the finishing tests. Surface morphologies variation with processing time change is observed by a metalloscope (Axio Lab A1). The surface topography in successive finishing trials is shown in Fig. 10. Some obvious scratches are created on the initial surface by sanding as shown in Fig. 10a. The scratches were eliminated with the increase of processing time, as shown in Fig. 10 b and c. The surface quality has a clear improvement by comparing the initial surface after 90 min finishing, as shown in Fig. 10d.

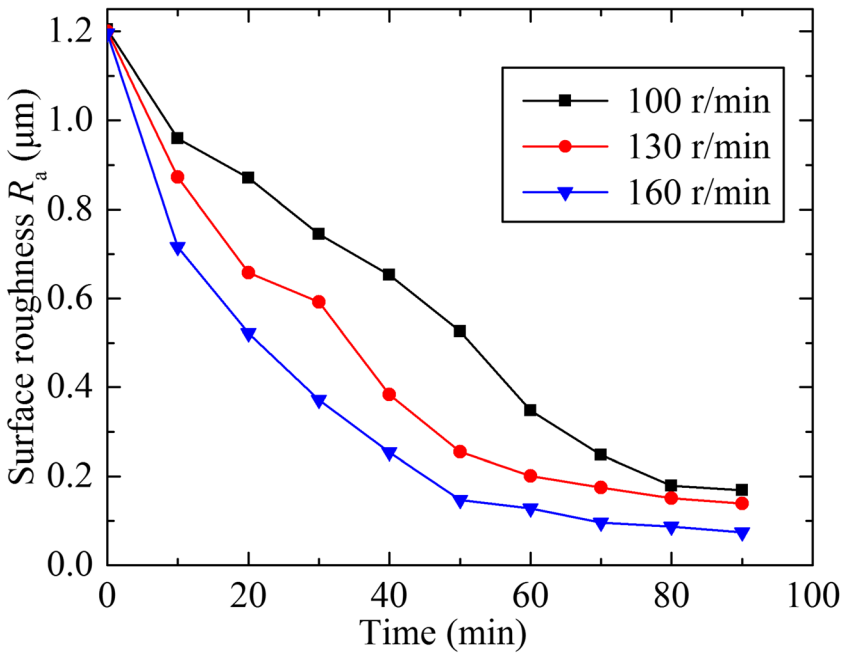

Fig. 8 Surface roughness variation with different rotary table speeds

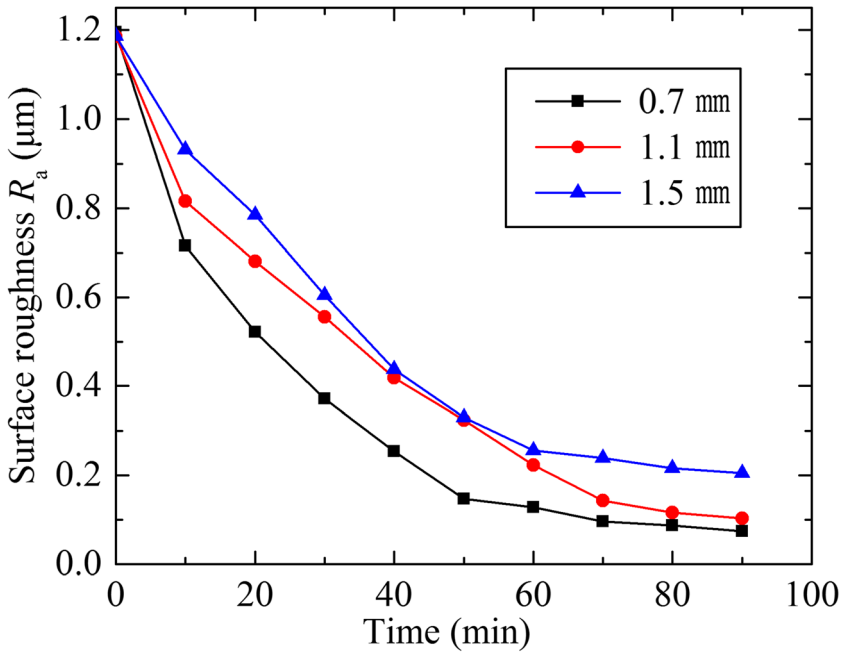

Fig. 9 Surface roughness variation with different working gap sizes

The finished surface characteristics and texture were investigated by a field-emission scanning electron microscopy (FEI Sirion 200). Figure 11 shows the surface changes in physical picture and SEM observations before and after finishing processes. The initial surface characterized by deep scratches is shown in Fig. 11a. And there were some melted–solidified layer on the initial surface caused by wire electrical discharge machining (WEDM). A smooth surface without obvious scratches and melted–solidified layer was obtained, as shown in Fig. 11b. It is clearly demonstrated that there is an obvious improvement in surface characteristic of the finished surface. This conforms that the designed finishing tool is effective of removing the peaks of the workpiece. Some shallow grinding marks were left on the finished surface because of the friction of abrasive. The fine abrasive grains can be adopted for the further removal of grinding marks. This means coarse grain abrasives are beneficial for better material removal at the beginning of the finishing process.

Figure 12 shows the SEM micrographs of abrasive media before and after finishing. The SiC abrasive particles have cutting edges held by carbonyl iron particles, as shown in Fig. 12a. The peaks were sheared from the workpiece surface when abrasive media were moved relatively to the workpiece surface. After finishing, some carbonyl iron particles were ground, and the cutting edges of SiC particles became blunt. Besides, some titanium alloy chips appeared in the finished abrasive media, as shown in Fig. 12b. The amount of material removal from the workpiece surface relies on the experimental conditions. Experimental results indicate that the developed finishing tool is feasible for Ti-6Al-4V finishing regarding surface roughness and topography, which is clearly shown by investigating the variation in the surface roughness and characteristics.

6 Conclusions

An improved finishing tool with integrated multiple magnetic poles was designed for surface finishing. Finite element analysis of the variation of field intensity in the finishing fields indicates formation of magnetic brush using the commercial

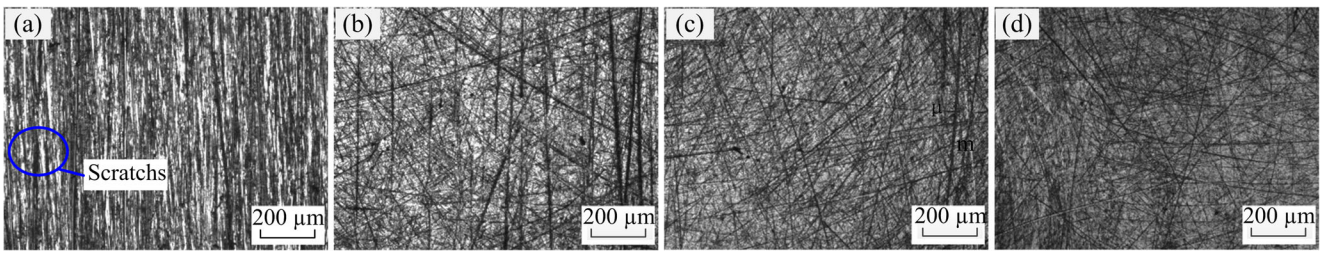

Fig. 10 Surface topography with various time. **a** 0 min, **b** 30 min, **c** 60 min, and **d** 90 min

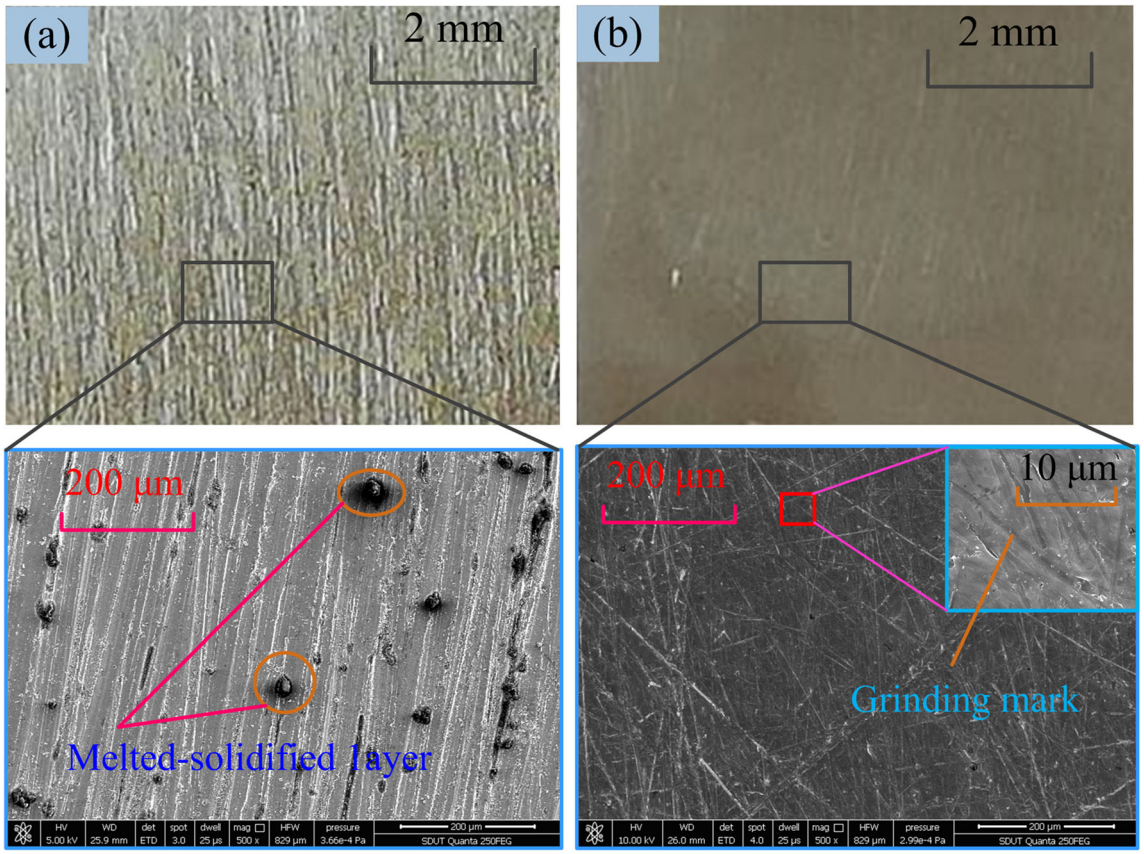

Fig. 11 Physical and SEM micrographs of a workpiece **a** before and **b** after finishing

Maxwell software. The N-S-N mode of multiple permanent magnets is arranged for the developed finishing tool. The contrast experiments show that the variation tendency of the experimental results is consistent with simulation results in field intensity changing. A prototype of the finishing tool was manufactured. The feasibility of the designed tool was experimentally verified by extensive finishing experiments for Ti-6Al-4V workpieces. The surface roughness of finished surface was dominated by the spindle rotational speed, rotary table speed, and working gap size. Final surface roughness value of 0.073 μm was achieved from initial 1.195 μm under the experimental conditions of 900-rpm spindle rotational speed, 160 r/min rotary table speed, and 0.7-mm working gap in 90 min. The capability of the developed finishing tool to improve the surface characteristics of Ti-6Al-4V workpiece was investigated via SEM and metalloscope observations. The results showed that a smooth surface without obvious scratches was achieved after finishing. It was further confirmed that the developed finishing tool was capable of performing the nano-finishing on Ti-6Al-4V workpiece.

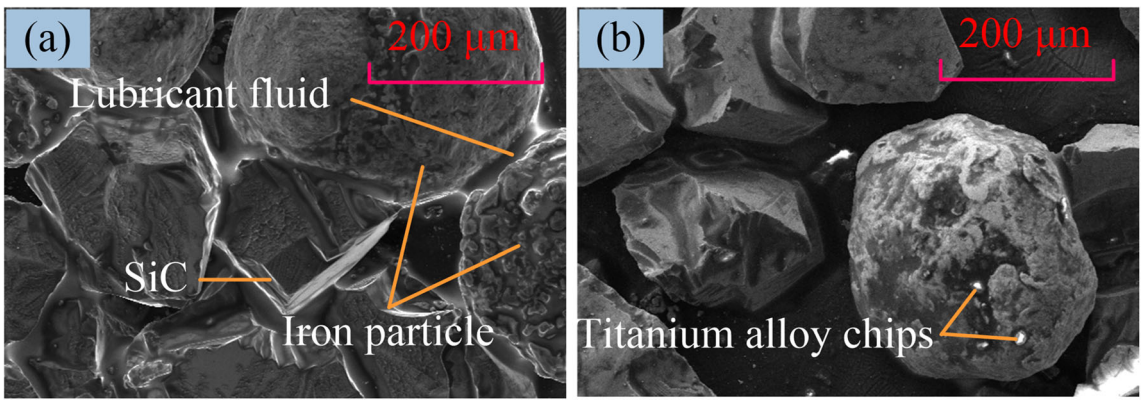

Fig. 12 SEM micrographs of abrasive media **a** before and **b** after finishing

Funding information This research work was supported by the National Natural Science Foundation of China (Grant No. 51875329 and 51905323), Taishan Scholar Special Foundation of Shandong Province (Grant No. tsqn201812064), Shandong Provincial Natural Science Foundation, China (Grant No. ZR2017MEE050 and ZR2017QEE003), Shandong Provincial Key Research and Development Project, China (Grants No. 2018GGX103008), Scientific Innovation Project for Young Scientists in Shandong Provincial Universities (Grant No. 2019KJB030), and Key Research and Development Project of Zibo City (Grant No. 2019ZBXC070).

References

1. Polishetty A, Littlefair G, Praveen KK (2014) Machinability assessment of titanium alloy Ti-6Al-4V for biomedical applications. Adv Mater Res 941-944(5):1985–1990. https://doi.org/10.4028/www.scientific.net/AMR.941-944.1985
2. Boyer RR (1996) An overview on the use of titanium in the aerospace industry. Mat Sci Eng A 213(1–2):103–114. https://doi.org/10.1016/0921-5093(96)10233-1
3. Mingareev I, Bonhoff T, El-Sherif AF, Richardson M (2013) Femtosecond laser post-processing of metal parts produced by laser additive manufacturing. J Laser Appl 25(5):052009. https://doi.org/10.1051/matecconf/20130802010
4. Lamikiz A, Sánchez JA, López de Lacalle LN, Arana JL (2007) Laser polishing of parts built up by selective laser sintering. Int J Mach Tools Manuf 47(12–13):2040–2050. https://doi.org/10.1016/j.ijmachtools.2007.01.013
5. Kim JS, Lim ES, Jung YG (2012) Determination of efficient superfinishing conditions for mirror surface finishing of titanium. J Cent South Univ 19(1):155–162. https://doi.org/10.1007/s11771-012-0985-6
6. Okada A, Uno Y, Yabushita N, Uemura K, Raharjo P (2004) High efficient surface finishing of bio-titanium alloy by large-area electron beam irradiation. J Mater Process Tech 149(1–3):506–511. https://doi.org/10.1016/j.jmatprotec.2004.02.017
7. Amnieh SK, Mosaddegh P, Tehrani AF (2017) Study on magnetic abrasive finishing of spiral grooves inside of aluminum cylinders. Int J Adv Manuf Technol 91(5):1–10. https://doi.org/10.1007/s00170-016-9970-9
8. Beaucamp AT, Namba Y, Charlton P, Jain S, Graziano AA (2015) Finishing of additively manufactured titanium alloy by shape adaptive grinding (SAG). Surf Topogr-Metrol 3(2):024001. https://doi.org/10.1088/2051-672X/3/2/024001
9. Revankar GD, Shetty R, Rao SS, Gaitonde VN (2014) Analysis of surface roughness and hardness in ball burnishing of titanium alloy. Measurement 58:256–268. https://doi.org/10.1016/j/measurement.2014.08043
10. Axinte DA, Kritmanorot M, Axinte M, Gindy NNZ (2005) Investigations on belt polishing of heat-resistant titanium alloys. J Mater Process Tech 166(3):398–404. https://doi.org/10.1016/j.jmatprotec.2004.08.030
11. Zhu D, Luo S, Yang L, Chen W, Yan S, Ding H (2015) On energetic assessment of cutting mechanisms in robot-assisted belt grinding of titanium alloys. Tribol Int 90:55–59. https://doi.org/10.1016/j.triboint.2015.04.004
12. Ohmori H, Katahira K, Mizutani M, Komotori J (2004) Investigation on color-finishing process conditions for titanium alloy applying a new electrical grinding process. CIRP Ann-Manuf Techn 53(1):455–458. https://doi.org/10.1016/S0007-8506(07)60738-0
13. Liang C, Liu W, Li S, Kong H, Zhang Z, Song Z (2016) A nanoscale mirror-like surface of Ti-6Al-4V attained by chemical mechanical polishing. Chinese Phys B 25(5):58301–058301. https://doi.org/10.1088/1674-1056/25/5/058301
14. Ozdemir Z, Ozdemir A, Basim GB (2016) Application of chemical mechanical polishing process on titanium based implants. Mat Sci Eng C Mater 68:383–396. https://doi.org/10.1016/j.msec.2016.06.002
15. Wojciech S, Michat M, Ginter N, Pawel N, Jerzy Z, Jacek S, Antoni W, Artur M, Szyk-Warszynska L (2012) Electrochemical polishing of Ti–13Nb–13Zr alloy. Surf Coat Tech 213(12):239–246. https://doi.org/10.1016/j.surfcoat.2012.10.055
16. Huang P, Lai J, Han L, Yang F, Jiang L, Su J, Tian Z, Tian Z, Zhan D (2016) Electropolishing of titanium alloy under hydrodynamic mode. Sci China Chem 59(11):1525–1528. https://doi.org/10.1007/s11426-016-0211-y
17. Guo J, Tan ZE, Au KH, Liu K (2017) Experimental investigation into the effect of abrasive and force conditions in magnetic field-assisted finishing. Int J Adv Manuf Technol 90(5–8):1881–1888. https://doi.org/10.1007/s00170-016-9491-6
18. Zou Y, Xie H, Dong C, Wu J (2018) Study on complex micro surface finishing of alumina ceramic by the magnetic abrasive finishing process using alternating magnetic field. Int J Adv Manuf Technol 97(5–8):2193–2202. https://doi.org/10.1007/s00170-018-2064-0
19. Umehara N, Kirtane T, Gerlick R, Jain VK, Komanduri R (2006) A new apparatus for finishing large size/large batch silicon nitride (Si3N4) balls for hybrid bearing applications by magnetic float polishing (MFP). Int J Mach Tools Manuf 46(2):151–169. https://doi.org/10.1016/j.ijmachtools.2005.04.015
20. Das M, Jain VK, Ghoshdastidar PS (2012) Nanofinishing of flat workpieces using rotational–magnetorheological abrasive flow finishing (R-MRAFF) process. Int J Adv Manuf Technol 62(1–4):405–420. https://doi.org/10.1007/s00170-011-3808-2
21. Kheelraj P, Pulak MP (2018) Use of chemical oxidizers with alumina slurry in double disk magnetic abrasive finishing for improving surface finish of Si (100). J Manuf Process 32:138–150. https://doi.org/10.1016/j.jmapro.2018.02.007
22. Singh AK, Jha S, Pandey PM (2012) Nanofinishing of a typical 3D ferromagnetic workpiece using ball end magnetorheological finishing process. Int J Mach Tools Manuf 63:21–31. https://doi.org/10.1016/j.ijmachtools.2012.07.002
23. Barman A, Das M (2017) Design and fabrication of a novel polishing tool for finishing freeform surfaces in magnetic field assisted finishing (MFAF) process. Precis Eng 49:61–68. https://doi.org/10.1016/j.precisioneng.2017.01.010
24. Barman A, Das M (2019) Toolpath generation and finishing of bio-titanium alloy using novel polishing tool in MFAF process. Int J Adv Manuf Technol 100:1123–1135. https://doi.org/10.1007/s00170-017-1050-2
25. Zhou K, Chen Y, Du ZW, Niu FL (2015) Surface integrity of titanium part by ultrasonic magnetic abrasive finishing. Int J Adv Manuf Technol 80(5–8):997–1005. https://doi.org/10.1007/s00170-015-7028-z
26. Parameswari G, Jain VK, Ramkumar J, Nagdeve L (2019) Experimental investigations into nanofinishing of Ti6Al4V flat disc using magnetorheological finishing process. Int J Adv Manuf

Technol 100:1055–1065. https://doi.org/10.1007/s00170-017-1191-3

27. Yamaguchi H, Hendershot P, Pavel R, Iverson JC (2016) Polishing of uncoated cutting tool surfaces for extended tool life in turning of Ti–6Al–4V. J Manuf Process 24(2):355–360. https://doi.org/10.1016/j.jmapro.2016.06.014
28. Yamaguchi H, Srivastava AK (2012) Magnetic abrasive finishing of cutting tools for machining of titanium alloys. CIRP Ann-Manuf Technol 61(1):311–314. https://doi.org/10.1016/j.cirp.2012.03.066
29. Preston FW (1927) The theory and design of plate glass polishing machines. J Glass Technol 11(44):214–256
30. Sato T, Kum CW, Venkatesh VC (2013) Rapid magneto-rheological finishing of Ti-6Al-4V for aerospace components. Int J Nanomanuf 9(5–6):431–445. https://doi.org/10.1504/IJNM.2013.057590